Investigation of installation stress level on the vertical and lateral loading behaviour of open-ended piles by centrifuge tests

Li, Qiang; Ma, Qunchao; Cheng, Xinglei; Gavin, Kenneth; Prendergast, Luke J.; Askarinejad, Amin

DOI
10.1016/j.oceaneng.2025.121756

Publication date
2025

Document Version
Final published version

Published in
Ocean Engineering

Citation (APA)
Li, Q., Ma, Q., Cheng, X., Gavin, K., Prendergast, L. J., & Askarinejad, A. (2025). Investigation of installation stress level on the vertical and lateral loading behaviour of open-ended piles by centrifuge tests. *Ocean Engineering*, *335*, Article 121756. https://doi.org/10.1016/j.oceaneng.2025.121756

Ocean Engineering 335 (2025) 121756

Contents lists available at ScienceDirect

Ocean Engineering

journal homepage: www.elsevier.com/locate/oceaneng

Research paper

Investigation of installation stress level on the vertical and lateral loading behaviour of open-ended piles by centrifuge tests

Qiang Li [a], Qunchao Ma [b], Xinglei Cheng [c,*], Kenneth Gavin [d], Luke J. Prendergast [e], Amin Askarinejad [d]

[a] PowerChina Huadong Engineering (Shenzhen) Corporation limited, Shenzhen, China
[b] School of Civil Engineering, Zhejiang University of Technology, Hangzhou, China
[c] Key Laboratory of Soft Soil Engineering Character and Engineering Environment of Tianjin, Tianjin Chengjian University, Tianjin, China
[d] Faculty of Civil Engineering and Geosciences, Delft University of Technology, Delft, the Netherlands
[e] Department of Civil Engineering, Faculty of Engineering, University of Nottingham, Nottingham, United Kingdom

ARTICLE INFO

Keywords:
Open-ended piles
Centrifuge tests
Loading behaviours
Installation stress level
Soil plug effect

ABSTRACT

Extensive research has focused on quantifying the loading behaviour of 1*g* (*g*, gravitational acceleration rate) installed open-ended piles using centrifuges. However, the influence of installation stress level on loading behaviour is often ignored, with ramifications for the accuracy and validity of results. In this paper, a loading apparatus is developed to allow in-flight jacking of piles followed directly by vertical or lateral loading, without needing to stop the centrifuge, which facilitates maintaining the installation-related stress state. Model piles are installed at 50*g* and 1*g*, and the vertical and lateral responses are analyzed. The effect of pile installation stress level on the initial stiffness, resistance, and soil plug behaviour, is investigated. Results indicate that installation stress level has a more significant and non-uniform effect on pile vertical behaviour than lateral behaviour. Piles that are not fully installed at 50*g* can mobilize the same vertical resistance as those fully installed at 50*g*, provided they experience a minimum of 2*D* (*D*, pile diameter) in-flight installation length. The arching effect caused by soil plugging, and the denser sand state surrounding the pile toe, may provide higher vertical and lateral resistance for piles installed at 50*g* compared to those installed at 1*g*.

List of notation

D	pile outer diameter	q_c	CPT end resistance
D_{10}	sieve opening corresponding to 10 percent finer by weight	q_{plug}	plug resistance
D_{50}	average grain size of sand	t	pile wall thickness
D_{60}	sieve opening corresponding to 60 percent finer by weight	u	pile vertical displacement
D_r	relative density of sand	V	vertical load
e	lateral load eccentricity	y	pile lateral displacement
e_{max}	maximum void ratio of sand	z	soil depth
e_{min}	minimum void ratio of sand	γ_{max}	maximum unit weight of sand
EI	bending stiffness	γ_{min}	minimum unit weight of sand
g	gravitational acceleration rate	τ_e	external shear stress on pile wall
g_0	initial stiffness in lateral load test	τ_i	internal shear stress on pile wall

(*continued on next column*)

(*continued*)

G_s	specific gravity	Δ	increase
H	lateral load	φ_{cv}	constant volume friction angle
k_0	initial stiffness in vertical load test	Φ	soil plug ratio
k_1	loading stiffness in vertical load test	DEM	discrete element method
L	pile embedment length	IFR	incremental filling ratio
L_p	length of soil plug	PFC2D	two-dimensional particle flow code
L_{up}	length of unwedged plug	MPM	material point method
L_{wp}	length of wedged plug	OWT	offshore wind turbine
P	soil reaction	SLS	serviceability limit state
q_{ann}	pressure at base of annulus	ULS	ultimate limit state

1. Introduction

Monopiles support more than 80 % of existing offshore wind turbines

* Corresponding author.
E-mail address: chengxinglei110@163.com (X. Cheng).

https://doi.org/10.1016/j.oceaneng.2025.121756
Received 13 September 2024; Received in revised form 9 May 2025; Accepted 2 June 2025
Available online 4 June 2025

(OWTs) (Cheng et al., 2022, 2023, 2025; Fan et al., 2019; Komusanac et al., 2021; Li et al., 2020a, 2020c, 2024a, 2024b). Monopile foundations consist of open-ended steel cylinders that are typically driven by hammers, or installed with vibration into the seabed. Typical monopiles have a diameter (D) of 4–8 m, a wall thickness (t) of 50–120 mm, and an embedment length (L) of 20–50 m, giving a slenderness ratio (L/D) of 4–6. These foundations have mainly been employed for OWTs in shallow water coastal regions with water depths ranging from approximately 10 m–35 m, supporting OWTs with power ratings of 2–8 MW (Sørensen and Ibsen, 2013; Wang et al., 2022). Recent OWTs have dramatically increased in their size and power generation capacity, with pile diameters exceeding 10 m, and capacities over 15 MW. These new systems are being deployed in water depths exceeding 60 m (Byrne, 2021; Ma et al., 2024).

Due to the large size of OWTs, prototype experimental testing is very challenging or impossible (Cheng et al., 2024). Alternative strategies adopted by various researchers include performing scaled model testing at 1g, centrifuge modelling, or establishing numerical models to understand system behaviour. Examples of scaled experimental testing include the recent Pile-Soil Analysis (PISA) project, whereby a modified p-y (soil reaction-pile displacement) method was developed by Byrne et al. (2019). PISA comprised onshore testing of driven piles (with a maximum diameter $D = 2$ m and an embedment length $L \leq 5.25D$) subjected to monotonic push-over loading in both sand and clay deposits. In another study, open-ended steel pipe piles ($L = 2.4$ m, $D = 0.6$ m) were installed into dense sand by means of impact and vibratory pile driving, and subjected to cyclic lateral loading (Stein et al., 2018). Pile driving predictions and measurements during the installation process were investigated. These scaled experimental trials are valuable, but are limited to the properties of the sites chosen, and do not experience the same stress conditions as full-scale systems.

Centrifuge testing offers an opportunity to investigate full-scale behaviour of geotechnical models at reduced scales, by maintaining similitude in stress conditions between the model and full-scale system (Li et al., 2020c; Zhu et al., 2019). The difficulty, cost, manpower, and time associated with full and pilot-scale experimental testing can be significantly reduced using this approach. Centrifuge testing usually involves simplifications for ease of modelling. One such simplification relates to how piles are typically installed. In the majority of published centrifuge tests relating to vertical and lateral pile behaviour (Askarinejad et al., 2022; Choo and Kim, 2016; Klinkvort and Hededal, 2013, 2014; Li et al., 2010a, 2022; Lu and Zhang, 2018; Mu et al., 2018; Richards et al., 2021; Qi et al., 2016; Truong et al., 2018; Verdure et al., 2003; Yang et al., 2019; Yoo et al., 2013), piles were installed at reduced g-levels by jacking, to simplify the testing procedure. As a result, the effect of installation-related stress levels on the subsequent loading responses was not taken into account. Pile jacking is used in centrifuge testing as a means to approximate pile installation by impact driving as would occur in the real case, due to the challenges typically associated with hammering a pile into the ground during centrifuge testing. Different pile jacking approaches have been adopted to simulate impact-driving installation. For example, Li et al. (2010b) compared three different pile jacking procedures: (i) “cyclic jacking”, where model piles were pressed into the soil in-flight at high “g”, with unload/reload cycles representing the repeated repositioning of the driving head similar to piles being driven in the field; (ii) “monotonic jacking”, where model piles were installed in-flight at high “g” without intermediate unload-reload cycles; and (iii) “pre-jacking”, where model piles were jacked at 1g prior to centrifuge spin-up. Although the last pile installation procedure does result in soil displacement, the consequential locked-in stresses were assumed to be very small, with the pile behaviour assumed to be similar to a bored pile in the field. The nature of how piles are installed can influence the subsequent modelled behaviour.

Design guidelines such as DNV (2014) acknowledge that the influence of installation method (and stress level) on the in-service behaviour of monopile foundations should be considered. The stress distribution in the surrounding soil can be significantly influenced by the monopile installation method (Henke and Bienen, 2013; Labenski et al., 2016), thus potentially affecting the subsequent vertical and lateral loading responses. In some cases where piles have been installed in-flight, application of subsequent lateral and vertical loading has necessitated stopping the centrifuge to adjust loading rigs, which adds uncertainty surrounding the influence of the sample stress history on the results obtained (Li et al., 2020b, 2022). Other previous research suggests that pile vertical loading responses are strongly influenced by the installation method (De Nicola and Randolph, 1997; Henke and Bienen, 2013; Mahutka et al., 2006), while lateral loading responses are apparently less affected (Fan et al., 2019; Wen et al., 2020, 2023, 2024a; Zhu et al., 2018), which suggests that there remains uncertainty surrounding the impact of the installation process on the subsequent vertical and lateral loading responses of open-ended piles in centrifuge tests.

Numerical studies of pile installation have been conducted by several researchers. Henke and Grabe (2008) and Labenski et al. (2016) simulated the installation process of piles in non-cohesive soil to investigate the effect of plugging under different installation methods, including quasi-static pile jacking, impact pile driving, and vibratory pile driving. Centrifuge experimental results were later used to validate the numerical model. Distributions of horizontal stress and zones of densification/loosening were revealed by the numerical analyses, which highlighted the differences resulting from the various installation methods. Phuong et al. (2016) applied the material point method (MPM), which is capable of modelling large deformations and soil-structure interaction, to simulate the pile installation process and subsequent static pile loading tests. Results suggested the installation of displacement piles in sand leads to large changes in the stress state, density, and soil properties around the pile tip and shaft; and therefore a significantly higher pile bearing capacity was observed during static load tests when comparing simulations with and without installation effects. Wen et al. (2024b) explicitly accounted for installation effects in the finite element simulation of axially loaded piles through dividing the soil domain into various regions. Duan et al. (2018) compared installation effects on a rigid driven pile and a rigid bored pile installed into an assembly of granular soil using a two-dimensional particle flow code (PFC2D) model of the discrete element method (DEM). It was found that the driven pile compressed the soil during the driving process thus performing better in the subsequent load tests. Furthermore, it was found that the driven pile and bored pile were influenced by the soil friction in different ways, specifically the soil friction exhibited an influence at the beginning of driving for the driven pile, while it only took effect after a certain installation depth for the bored pile. These numerical works develop representative computational approaches and provide predictions that can be benchmarked against experimental findings (Liu et al., 2024).

This paper investigates vertical and lateral loading behaviour of open-ended piles jacked into sand under different stress levels, i.e. 50g and 1g, in a centrifuge. Partial in-flight installation is also investigated to ascertain the influence on the mobilised stresses, with different 1g installation lengths trialled. Test results provide insights to the effect of installation stress level on the initial stiffness and ultimate resistance of piles, as well as reference criteria for experimental investigations and numerical simulations.

2. Development of experimental loading apparatus and test procedures

A two-dimensional actuator is used to impose vertical and lateral loads simultaneously or individually on structures in the centrifuge, as shown in Fig. 1. This loading system can apply two-dimensional loads under either load- or displacement-controlled conditions (Li et al., 2020b). Vertical and lateral displacements are monitored at each loading height by displacement encoders. All tests are performed as displacement-controlled in this paper, while the corresponding reaction

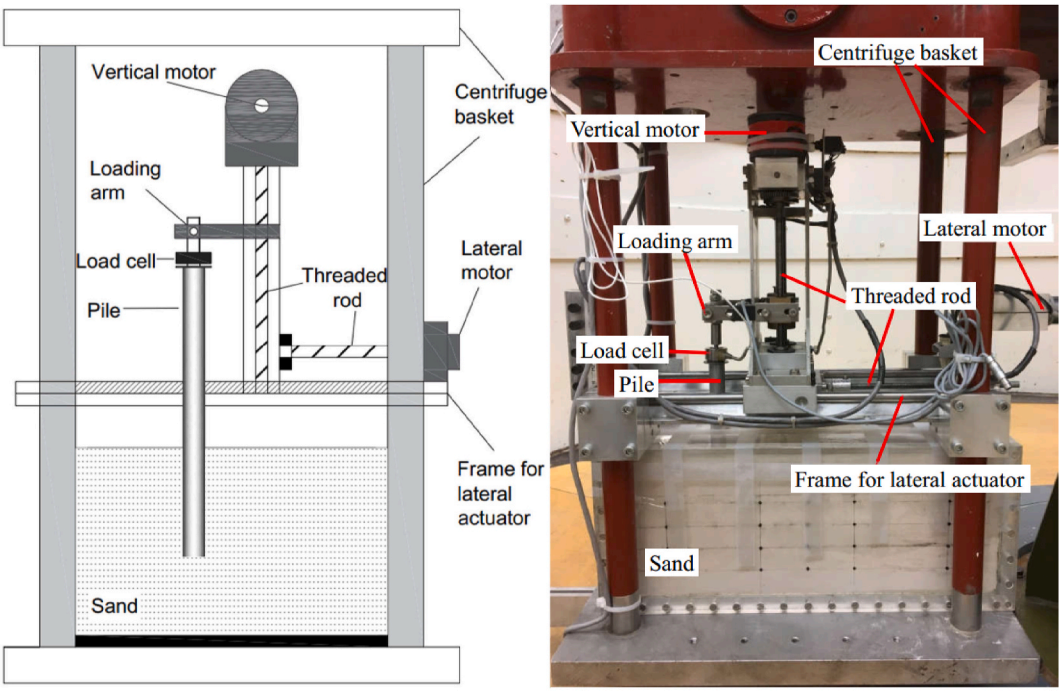

(a) (b)

Fig. 1. Two-dimensional loading actuator: (a) schematic diagram; (b) photo.

loads are measured by external load cells.

The experiments are classified in two categories by their loading characteristics, namely vertical loading, and lateral loading. Each category includes two phases, namely "pile installation phase" and "loading test phase". In the first phase, piles are designed to be either 50*g* installed or 1*g* installed by jacking, to investigate the influence of installation stress level on the subsequent loading behaviour. In the second phase, two distinct loading apparatuses (one for vertical loading, and one for lateral loading) are designed to fulfil the test requirements, as described in the following sections.

2.1. *Vertical loading apparatus*

2.1.1. *Piles installed at 50g and vertical load test*

Two loading arms are connected by a loading bar, as shown in Fig. 2. In the centre of the loading bar is a transition piece, the end of which is connected to a vertical load cell, with a measurement capacity of 5 kN (Model 8431-6005, Burster). A loading plate is attached to the bottom of

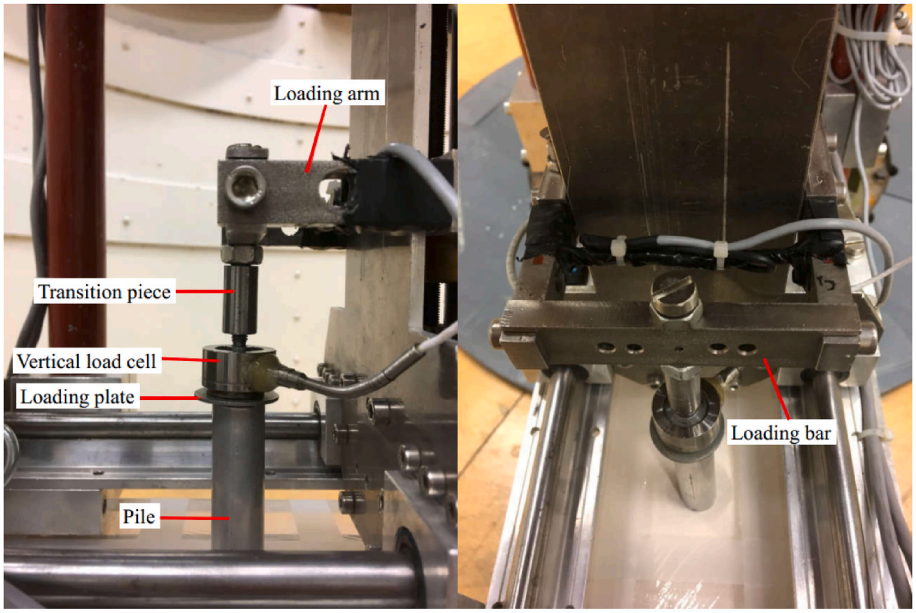

(a) (b)

Fig. 2. Vertical loading apparatus: (a) front view; (b) top-side view.

the vertical load cell to transfer the produced vertical load to the pile. The capacity of the vertical load cell was determined based on the force required to jack the pile, as justified by preliminary tests. The choice of 50*g* for the enhanced gravitational acceleration rate was determined by the ability to generate this jacking force, as higher gravitational acceleration rates require larger forces to jack piles in-flight. A jacking force of 4 kN (80 % of the vertical load cell capacity) is set as the upper limit to protect the two-dimensional loading frame.

In the experimental setup, the sand specimen is preliminarily placed into the centrifuge basket. The pile is placed vertically on the sand surface in its initial position (directly below the loading plate). The vertical actuator is subsequently moved downwards at a constant rate of 0.05 mm/s to install the pile, until the pile reaches an embedment depth of 2*D*. The pile toe is buried into the sand to keep the pile stable during the process of spinning up the centrifuge. The centrifuge ramps up from 1*g* to 50*g*, and remains at 50*g* for 120 s to produce and maintain the elevated stress level. Thereafter, the pile is further installed to the designed total embedment depth at a loading rate of 0.05 mm/s. Finally, the pile is unloaded to zero vertical load, thus completing the pile in-flight installation. By maintaining the centrifuge gravitational acceleration rate at 50*g*, the vertical loading test is then performed by re-activating the vertical actuator.

2.1.2. *Piles installed at 1g and vertical load test*

The procedure for installing the pile for the 1*g* tests is similar to that in the 50*g* tests. In this arrangement, the vertical actuator simply pushes the pile into the sand (at a rate of 0.05 mm/s) until it reaches its full embedment depth, where it is then unloaded. The centrifuge is then spun-up to 50*g* and held for 120 s, and subsequently the vertical loading test is performed by activating the vertical actuator.

2.2. *Lateral loading apparatus*

For the lateral loading tests, a loading block is installed between the two loading bars, as can be seen in Fig. 3. Fig. 4 schematically displays the lateral loading procedures including pile installation and lateral loading phases. The flat bottom of the loading block serves as a loading platform for pile installation, with front surface mounted with three parallel beam load cells (HTC-SENSORS; TAL220; each with measuring range of 100 N, sensitivity of 0.05 %), to measure lateral loads. An L-shaped loading plate is attached to the bottom of the parallel beam load cells to transfer the produced lateral load to the pile. The number and capacity of lateral load cells were determined through preliminary tests.

The installation methodology of the pile for the lateral loading tests is broadly the same as that in the vertical loading tests. It can be compared between Figs. 2 and 3 that the only differences are that: i) pile installation is accomplished by the loading block installed in between the two loading arms (Fig. 4a and b), rather than by the loading plate attached to the bottom of the vertical load cell; and ii) after pile installation, a clearance of 0.5*D* is created (Fig. 4c) between the pile top and the loading block by elevating the vertical actuator (releasing the pile head fixity) for the purpose of performing the lateral loading tests, while in the vertical loading tests this clearance is not required.

In-flight (at 50*g*), the lateral actuator is activated so that the L-shaped plate can push the pile laterally (Fig. 4d) at a constant rate of 0.05 mm/s, facilitating lateral load tests be performed. The lateral loading arrangement after testing is shown in Fig. 3b. The vertical and lateral loading rates were determined from centrifuge trial tests. A detailed description is presented in section 4.1.

3. Centrifuge model tests

3.1. *Centrifuge facility*

The experiments are undertaken using the beam centrifuge located in the Geo-Engineering laboratory at TU Delft. The centrifuge, with rotating arm of nominal diameter 2.5 m, has a maximum carrying capacity of 30 kg at a maximum gravitational acceleration rate of 300*g* (though this is limited in practice). More details are available in Refs. (Li et al., 2022; Zhang and Askarinejad, 2019).

3.2. *Model pile characteristics*

The model piles are open-ended cylindrical aluminium tubes with an outer diameter (*D*) of 18 mm, as schematically shown in Fig. 5. The pile diameter was selected to minimise boundary effects associated with the strong box. The strong box is fabricated from bolted Plexiglas with an inner dimension of 410 (length) × 150 (width) × 165 (height) mm^3. The

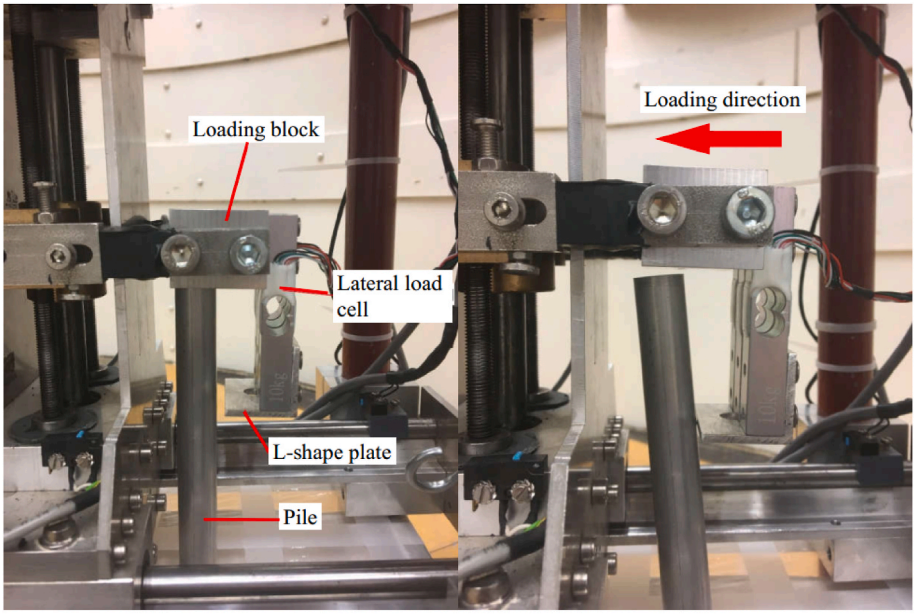

Fig. 3. Lateral loading apparatus: (a) pile installation arrangement; (b) lateral loading arrangement.

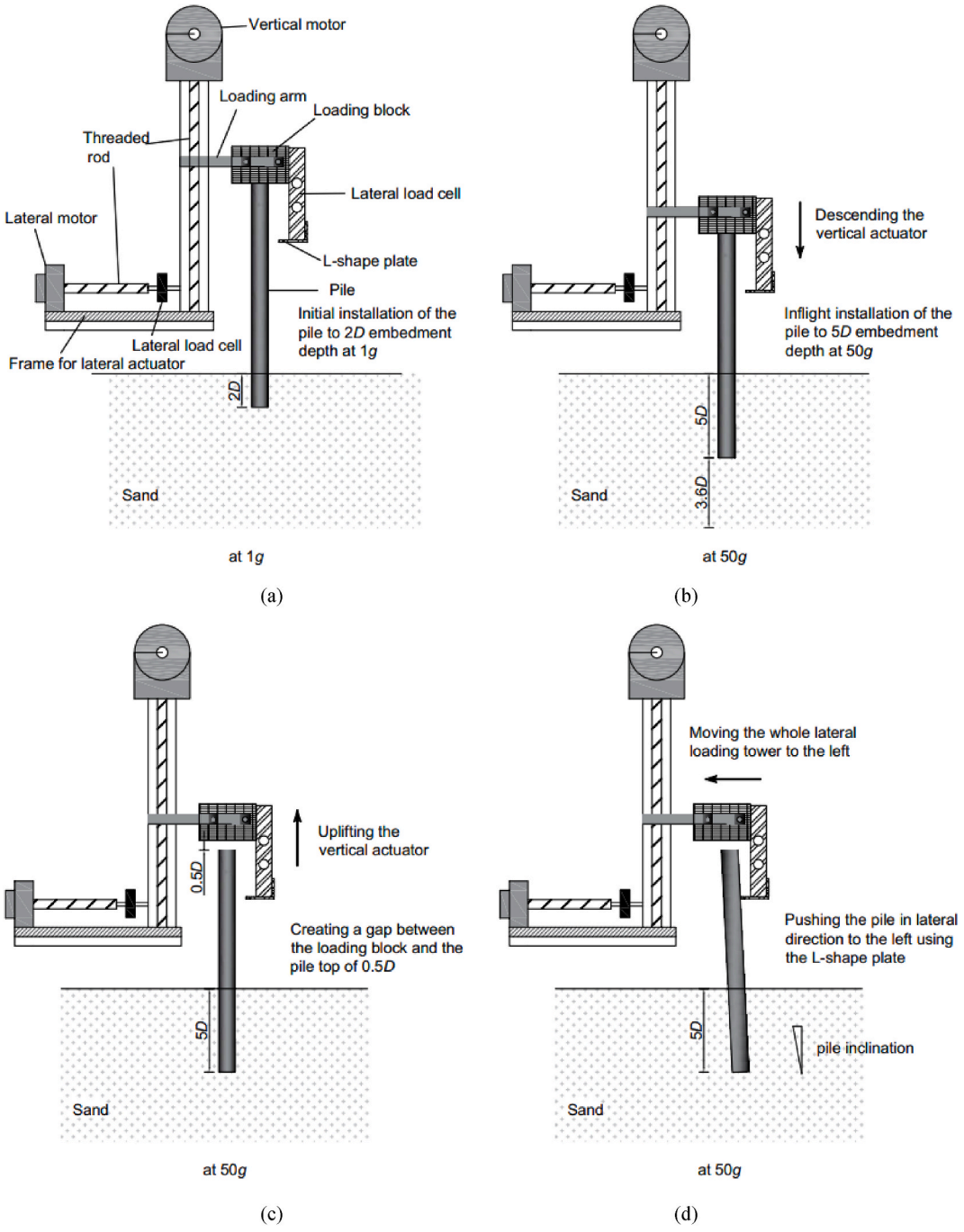

Fig. 4. Schematic of lateral loading procedures: (a) initial installation of the pile to 2*D* embedment depth at 1*g*; (b) in-flight installation of the pile to 5*D* embedment depth at 50*g*; (c) creation of a gap of 0.5*D* between the loading block and the pile top to release its restriction; (d) pushing the pile laterally by the L-shaped plate to perform lateral loading tests.

embedment length (L) of the pile is designed to give a slenderness ratio (L/D) of 5D, giving 90 mm. The sand layer is prepared with a maximum depth of 155 mm, and the distance from the pile toe to the bottom of the strong box in the tests is 3.6D (65 mm), avoiding the possible boundary effects (Prakasha et al., 2005).

The wall thickness (t) of the aluminium model pile is 1 mm at model scale, which corresponds to 0.3 mm in steel, derived based on the similitude between the bending stiffness (EI) of the prototype and the model (Gerolymos et al., 2009; Li et al., 2020b). Byrne et al. (2015) produced a database of piles used as OWT foundations, and presented the results of pile diameters normalised by wall thickness. For monopiles with an $L/D = 5$, the value of D/t normally varies from 39 to 80. In the present analysis, the D/t value for the steel prototype pile is 60, well within the expected range (Li et al., 2020b).

All load tests are performed at a gravitational acceleration rate of 50g to investigate installation effects. Therefore, the model pile properties represent an outer diameter (D) of 0.9 m, a wall thickness (t) of 50 mm (using aluminium material; equating to 15.2 mm in steel), an embedment (L) of 4.5 m, and a lateral loading eccentricity (e) of 7.2 m at the prototype scale (Fig. 5). The prototype dimensions are smaller than those typically used as OWT monopiles, which is a result of the limitations in the permissible pile geometry to avoid boundary effects, the capability of the two-dimensional loading frame, and the maximum acceleration field implemented in the centrifuge for the installation

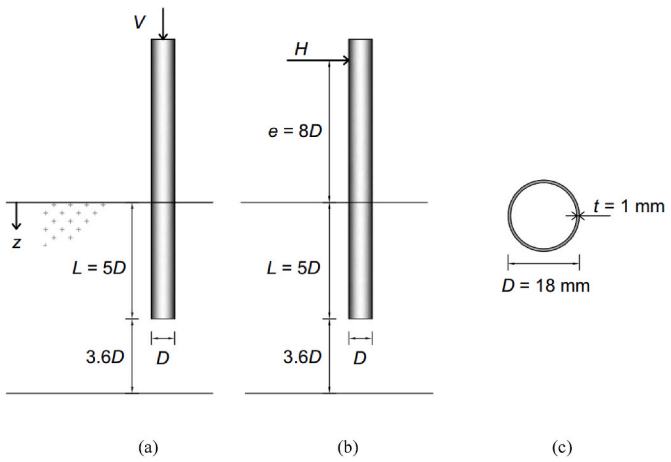

Fig. 5. Model pile schematic diagram: (a) vertical loading mode; (b) lateral loading mode; (c) pile cross-section.

testing. However, previous research has shown that it is the slenderness ratio (L/D) that governs the response of piles, rather than the absolute geometry (Byrne et al., 2015). The adopted L/D is within the typical range to model rigid open-ended piles for OWTs, mitigating the issue with the smaller diameter. It is therefore assumed that the pile will behave in line with expectations, regardless of the smaller absolute dimensions.

3.3. Soil preparation and characterization

Geba sand (SibelcoEurope, 2016), mainly comprised of silica (99 % SiO_2), is used in this study. 84.2 % of the sand grains have a diameter between 0.1 mm and 0.2 mm. From the grain size distribution curve (Fig. 6), it can be concluded that the Geba sand is poorly graded. According to Krapfenbauer (2016), the sand particles are mostly sub-rounded with high sphericity. The geotechnical parameters of Geba sand are provided in Table 1 (Li et al., 2022; Maghsoudloo et al., 2018).

As suggested by Ovesen (1979), the ratio of key structural dimensions to mean particle size of sand should not fall below 15. The ratio of the outer diameter of the pile to the mean particle size of Geba sand (D/D_{50}) is 163.6, which is sufficiently large to avoid particle size effects in the pile loading tests (Dyson and Randolph, 2001; Garnier et al., 2007; Klinkvort and Hededal, 2010; Li et al., 2022; Nunez et al., 1988; Zhang and Askarinejad, 2019). The ratio between the wall thickness of the pile and the mean particle size of Geba sand (t/D_{50}) in the present test program is 9.1, which is smaller than the case of $t/D_{50} = 11$ presented in De Nicola (1996) and De Nicola and Randolph (1997), but larger than the case of $t/D_{50} = 7.5$ presented in Verdure et al. (2003). Scaling issues related to the interaction between the pile annulus and soil particles can therefore be considered minimal.

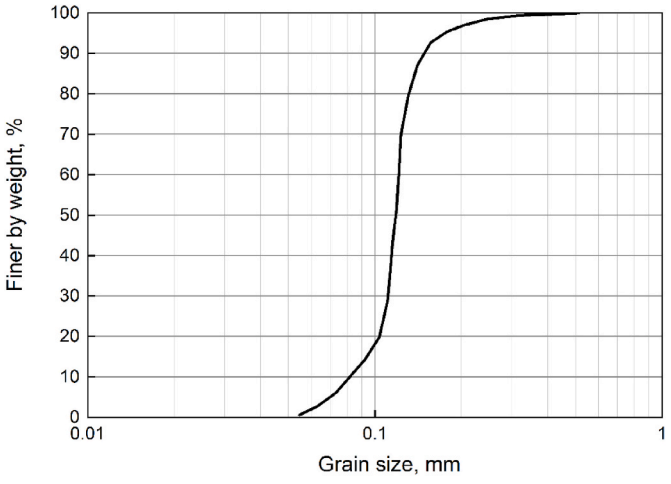

Fig. 6. Geba sand grain size distribution curve.

Dry sand was pluviated into the strong box using an automatic sand pouring machine (Li et al., 2020a), which consists of a storage tank holding sand, a trough hopper for pouring sand, and a height-adjustable bracket with rails that lifts the storage tank and trough hopper into place. The sand was prepared in the container in 5 mm layers. The relative density of each sand specimen was well-controlled and back-analyzed by the net weight of the sand box once filled. Reproducibility and homogeneity of each sand specimen was checked using X-ray scanning, ensuring reliable and uniform sand preparation.

The test pile was installed in the center of the container. The distance from the pile outer shaft to the nearest container boundary is 3.7D, larger than the limiting value of 2D as suggested by Prakasha et al. (2005). Two series of sand specimens with relative densities (D_r) of 80 % and 50 % were prepared to model dense and medium-dense states. The influence of water was not considered in the experimental trials conducted in this paper, representing a drained condition at prototype scale. While this is a simplification, the presence of water is not expected to alter the observed behavioural trends under low loading rates. Similar modelling strategies of using dry sand instead of saturated sand to mimic offshore environments in geotechnical experiments can be found in Klinkvort and Hededal (2013), LeBlanc et al. (2010), Li et al. 2010b, 2020b, Mu et al. (2018) and Verdure et al. (2003).

3.4. Test programme

The main centrifuge test programme comprises 12 tests, divided into 3 groups:

Group No. 1: Effect of in-flight installation length on the pile vertical resistance: 4 tests.

The piles with 1g installed lengths of 2D, 3D, 4D and 5D are 50g installed 3D, 2D, 1D and 0D (zero) lengths respectively to complete the installation process. Thereafter, all the piles are further vertically 50g jacked 1.3D-2.2D to evaluate the effect of in-flight installation length on the vertical resistance of the pile, and to explore the influence of boundary effects.

Group No. 2: Effect of stress level during installation on the vertical loading behaviour of piles: 4 tests.

The vertical load-displacement relationships are compared between 50g installed and 1g installed piles in dense and medium-dense sand respectively.

Group No. 3: Effect of stress level during installation on the lateral loading behaviour of piles: 4 tests.

The lateral load-displacement relationships are compared between 50g installed and 1g installed piles in dense and medium-dense sand, respectively.

A summary of the main tests conducted is given in Table 2. Additional tests that are performed for trial and comparison purposes (e.g., loading rate effects, repeatability checks) are not described in detail.

4. Analysis and results

4.1. Effect of loading rate and repeatability

The effect of loading rate on the mobilised vertical and lateral resistance of piles is evaluated herein. Vertical loading rates of 0.05 and 0.1 mm/s and lateral loading rates of 0.01, 0.05, 0.1, 0.1 (repeat), 0.2 mm/s (at model scale) are explored for tests T6 and T10 respectively. As can be seen in Fig. 7, the chosen loading rates have a minimal effect on the vertical and lateral loading stiffness and resistance behaviour. As a result, both the vertical and lateral loading rates are set at 0.05 mm/s for the remaining centrifuge tests.

Table 1
Geotechnical properties of Geba sand (Maghsoudloo et al., 2018; Askarinejad et al., 2022).

e_{min}	e_{max}	G_s	D_{10} (mm)	D_{50} (mm)	D_{60} (mm)	γ_{min} (kN/m^3)	γ_{max} (kN/m^3)	Roundness [-]	φ_{cv}
0.64	1.07	2.67	0.084	0.11	0.123	12.9	16.3	0.77	34°

Table 2
Details of the main centrifuge tests.

Test number	Sand relative density (D_r)	1*g* installed length	50*g* installed length	Vertical loading phase	Lateral loading phase
T1	80 %	2*D*	3*D*	2.2*D* jacking	–
T2	80 %	3*D*	2*D*	2.1*D* jacking	–
T3	80 %	4*D*	1*D*	2*D* jacking	–
T4	80 %	5*D*	–	1.3*D* jacking	–
T5 (50*g* installed)	80 %	2*D*	3*D*	1.5*D* jacking	–
T6 ([a]1*g* installed)	80 %	5*D*	–	1.3*D* jacking	–
T7 ([a]50*g* installed)	50 %	2*D*	3*D*	1.3*D* jacking	–
T8 ([a]1*g* installed)	50 %	5*D*	–	1.2*D* jacking	–
T9 ([a]50*g* installed)	80 %	2*D*	3*D*	–	1*D* pushing
T10 ([a]1*g* installed)	80 %	5*D*	–	–	0.9*D* pushing
T11 ([a]50*g* installed)	50 %	2*D*	3*D*	–	0.8*D* pushing
T12 ([a]1*g* installed)	50 %	5*D*	–	–	0.7*D* pushing

[a] The naming convention for 50*g* and 1*g* installed piles is based on whether there is 50*g* installed length during the pile installation phase.

4.2. Effect of pile in-flight installation length on vertical load-displacement relationships

Fig. 8 shows the vertical load-displacement relationships of the piles considering different 50*g* installation lengths. Dense sand (D_r = 80 %) specimens are used. Initial vertical stiffness (k_0, as shown in Fig. 8) of 10, 12.5, 16, and 20 MN/*D* is measured for piles with 50*g* installed lengths of 3*D*, 2*D*, 1*D* and 0*D* (zero). The larger 1*g* installed length the pile has, the higher the k_0 observed. After about 0.5*D* 50*g* installation, the stiffness decreases, and pile penetration resistance increases with the increase of vertical displacement at a comparatively constant rate. The unloading stiffness in the four cases is broadly similar, even though test T4 reaches a much smaller final displacement (6.3*D*) and lower final vertical resistance (6.1 MN), compared with the other three cases (at approximately 7.2*D* and 8.5 MN).

Regardless of the different 1*g* installation lengths, the vertical load-displacement curves begin to coincide after a vertical displacement of 6*D* for tests T1, T2 and T3, signifying that in-flight installation length has a limited effect on the mobilised ultimate vertical resistance of the piles (provided a minimum in-flight installation is achieved). It can be concluded from T3 that a minimum in-flight installation length of 2*D* is sufficient for the pile to mobilize the desired vertical resistance. The pile in T4 is 50*g* loaded to a vertical displacement of 1.15*D*, and then unloaded-reloaded to 1.3*D*, therefore it is not possible to say if it ultimately behaves with the same resistance as the other piles.

The vertical load-displacement relationships of T1, T2, and T3 remain steady before a total vertical displacement of 6.2*D*, increasing abruptly at the same rate after this point (u = 6.2*D*). The reason for this relates to boundary effects with the strong box, whereby when the piles are 6.2*D* embedded, the clearance between the pile toe and the bottom of the strong box is 2.4*D*. It is reasonable to suggest that 2.4*D* could be regarded as the lower limiting value to avoid boundary effects in vertical load tests of open-ended piles in sand using a geo-centrifuge, under the present modelling conditions.

4.3. Effect of pile installation stress level on the vertical loading behaviour

In the following vertical and lateral loading tests where pile in-flight installation is undertaken, piles are 1*g* installed for 2*D* length, then 50*g* installed another 3*D* length, fulfilling the 5*D* pile installation length in total. The effect of stress level during installation on the vertical loading behaviour of piles in both dense sand and medium dense sand is shown in Fig. 9.

4.3.1. Dense sand

The initial vertical stiffness k_0 (as shown in Fig. 9) for both 50*g* installed (T5) and 1*g* installed (T6) piles is the same, at approximately 12 MN/*D*. The vertical load-displacement curve of the 50*g* installed pile exhibits much higher vertical stiffness k_1 (as shown in Fig. 9) than that of the 1*g* installed pile, from 0 to 0.33*D*, due to the high pile installation stress level and the previous unloading-reloading effect. The vertical load-displacement curve of the 50*g* installed pile shows a k_1 of around 10 MN/*D* within the first vertical displacement of 0.33*D*, then k_1 reduces suddenly to about 1 MN/*D* for the remaining pile penetration. For the 1*g* installed pile, the vertical load increases continuously with vertical displacement without an abrupt change in k_1.

The vertical load-displacement curve of the 50*g* installed pile coincides with the 1*g* installed pile at a vertical displacement of 1.5*D*, aligning with the finding in section 4.2. At the same vertical displacement, the vertical resistance of both the 50*g* and 1*g* installed piles in dense sand are about three times those in medium-dense sand.

4.3.2. Medium-dense sand

As in the dense sand case, k_0 is similar for both 50*g* installed (T7) and 1*g* installed (T8) piles, at approximately the same value as that in dense sand (12 MN/*D*). The vertical load-displacement curve of the 50*g* installed pile shows a much higher k_1 than that of the 1*g* installed pile, due to the high pile installation stress level. The vertical load-displacement curve of the 50*g* installed pile shows a k_1 of around 12 MN/*D* within the first vertical displacement range of 0.13*D*, with k_1 then reducing suddenly to about 0.7 MN/*D* for the remaining pile penetration. For the 1*g* installed pile, the vertical load increases continuously with vertical displacement without an abrupt change in k_1, similar to the observation in dense sand.

In medium dense sand, the vertical resistance at 0.1*D* of the 50*g* installed pile is 1.2 MN, about twice that of the 1*g* installed pile (0.6 MN), as shown in Fig. 9. The traditional vertical load capacity criteria (vertical load at 0.1*D* vertical displacement, Lee, 2008) shows some discrepancy in the vertical capacities calculated in medium-dense and dense sand, which requires further analyses. Moreover, the vertical load-displacement curves of the 50*g* installed pile coincide with the 1*g* installed pile at about 2*D*, which echoes the findings in section 4.2 and 4.3.1. When comparing the 1*g* installed piles (T6 and T8), k_1 in dense sand is about twice that in medium dense sand.

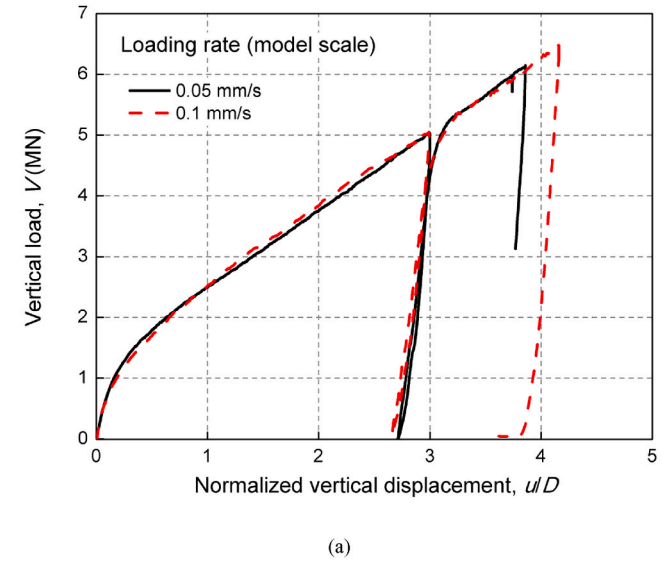

Fig. 7. Effect of loading rate on pile behaviour: (a) vertical load-displacement relationships; (b) lateral load-displacement relationships (D_r = 80 %).

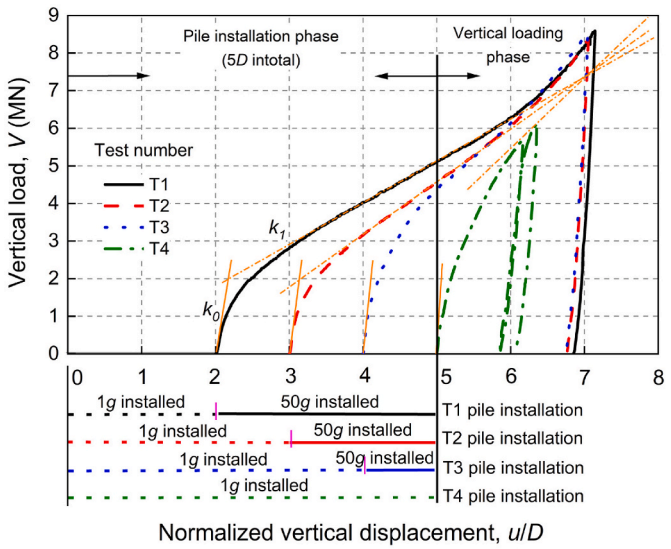

Fig. 8. Effect of pile in-flight installation length on the vertical load-displacement relationships (D_r = 80 %). (The dash-dot-dash extension line shows the possible intersection position of the piles with different in-flight installation lengths).

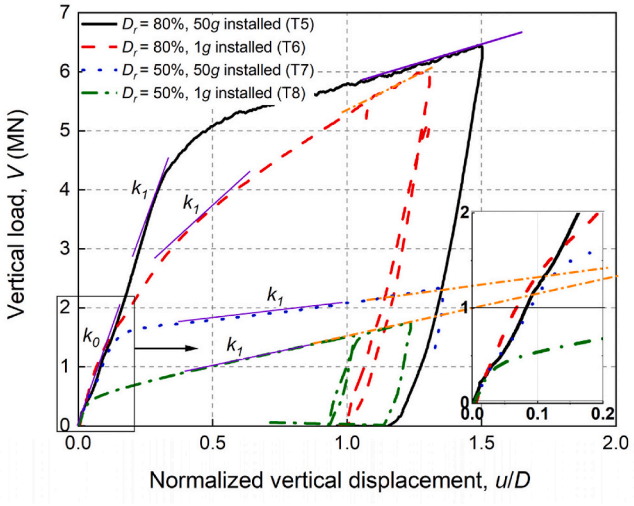

Fig. 9. Effect of pile installation stress level on the vertical loading behaviour. (The dash-dot-dash extension line shows the possible intersection position of the 50*g* installed pile and 1*g* installed pile through linear projection).

4.4. *Effect of pile installation stress level on the lateral loading behaviour*

Fig. 10 presents the effect of installation stress level on the lateral loading behaviour of piles, and it can be seen that the installation stress level has an equally important effect on the lateral load-displacement behaviour of piles in dense and medium-dense sand. When sand density is in a certain state (dense or medium-dense), the initial lateral stiffness g_0 (as shown in Fig. 10) of the 50*g* installed pile is similar to that of the 1*g* installed pile. g_0 in dense and medium-dense sand are 3 MN/*D* and 1.5 MN/*D*, respectively. Within the initial loading displacement of 0.05*D* in dense sand and 0.1*D* in medium dense sand, installation stress level has no significant effect on the lateral resistance. With the increase of lateral displacement, the lateral resistance of the 50*g* installed piles is generally 11 % higher than that of the 1*g* installed piles in both dense and medium-dense sand, in agreement with the phenomenon observed by Fan et al. (2019). At the same lateral displacement, the resistance in dense sand is about twice that in the medium-dense sand, for both the 50*g* and 1*g* installed piles.

Comparing Figs. 9 and 10, it can be concluded that installation stress level affects vertical loading behaviour more significantly and non-uniformly, but it is not the same case for lateral loading behaviour. Therefore, in some cases, it might be reasonable to ignore the effect of installation stress level in the analysis of lateral loading behaviour of piles on the condition that the same installation technique (jacking method, for example) has been employed.

4.5. *Effect of pile installation stress level on soil plugging*

By measuring the height of the inner sand surface and pile embedment (L), soil plug length (L_P) can be calculated, as shown in Fig. 11. Soil plug length is firstly measured at the end of the 1*g* installation (of piles in T1 and T4), as summarized in Table 3. At the end of the 50*g* installation, the pile in T1 had a final embedment length of 5*D* and the soil plug length (L_P) was re-measured. The effect of installation stress level on the soil plug length (L_P) is explored herein. Notably, the soil plug ratio (Φ, $\Phi = L_P/L$) for the 50*g* installed pile (in T1) is observed to be smaller than that of the 1*g* installed pile (in T4), indicating that the elevated installation stress level caused by enhanced centrifuge gravitational

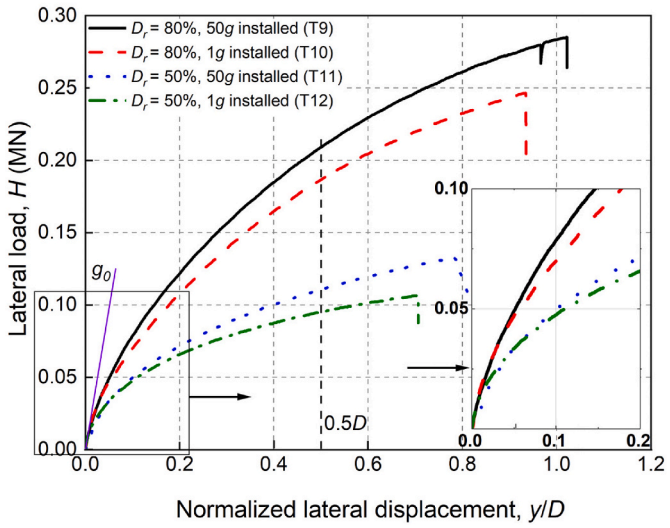

Fig. 10. Effect of pile installation stress level on the lateral loading behaviour. (The dash-dot-dash extension line shows the possible intersection position of the 50*g* installed pile and 1*g* installed pile).

acceleration rate is conducive to the formation of soil plugging. The smaller sand volume formulated within the "soil plug" of the 50*g* installed pile may mean a denser sand state was formed around the surfaces of the pile toe and the bottom of the sand plug. This phenomenon could potentially contribute to the increased vertical and lateral stiffness and resistance when piles are installed at higher stress levels. The total soil plug ratio of 0.6 for the pile in T1 is comparable to the ratio of 0.466 obtained by De Nicola and Randolph (1997) at the same penetration length (5*D*, D = 1.8 m) by using a similar pile and soil arrangement.

Furthermore, after removing the pile in T1, a dome shape is formed by the plugged sand, which had the ability to remain stable, as depicted in Fig. 12. This indicates that the dry sand particles especially at the bottom part of the pile were densely compressed. According to Lehane and Gavin (2001), the soil plug inside a pile is composed of an "unwedged plug" and a "wedged plug", as illustrated in Fig. 13. The "unwedged plug" exists in the upper layer of the soil core, providing little to no contribution to the plug resistance, or can even be regarded as a surcharge (Randolph et al., 1991). The "wedged plug", on the other hand, could provide plug resistance (q_{plug}). q_{plug}/q_c (q_c, cone tip resistance measured from a Cone Penetration Test, CPT) typically increases as IFR (incremental filling ratio, IFR = $\Delta L_P/\Delta L$; Δ, change) reduces and vice versa, which is consistent with the continual collapse and re-forming of sand arches during pile installation. In contrast, the dome shape was not observed when examining the piles that were solely 1*g* installed (i.e., in T4).

The formation of the soil plug and the resulting higher post-installation soil stress state near the pile column leads to higher vertical resistance, which results in a prominent difference between the 50*g* installed piles and the 1*g* installed piles in the vertical loading tests. In contrast, soil plug effects may not play such a substantive role on the lateral loading behaviour, as the difference between the 50*g* installed piles and the 1*g* installed piles is less significant.

5. Conclusions

In this study, the impact of jacking stress level (*g*-level) on the loading response features of open-ended piles is investigated using centrifuge modelling. A series of pile installation, vertical loading, and

Table 3
Effect of in-flight installation length on soil plugging.

Test number	Installed length at 1*g* [a]	Plug length [b]/ratio	Installed length at 50*g* [c]	Plug length [d]/ratio	Total plug length [e]/ ratio [f]
T1	2*D*	1.46*D*/ 0.73	3*D*	1.54*D*/ 0.51	3*D*/0.6
T4	5*D*	3.25*D*/ 0.65	–	–	3.25*D*/0.65

*e = b + d; f = e/(a + c).

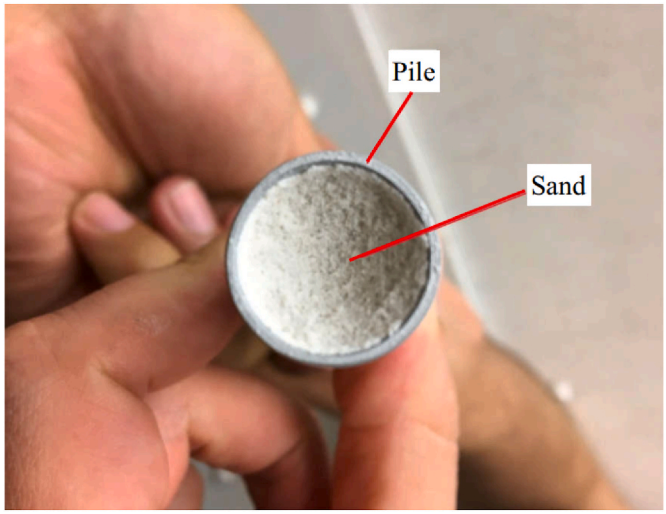

Fig. 12. Dome shape observed on the 50*g* installed pile (bottom view).

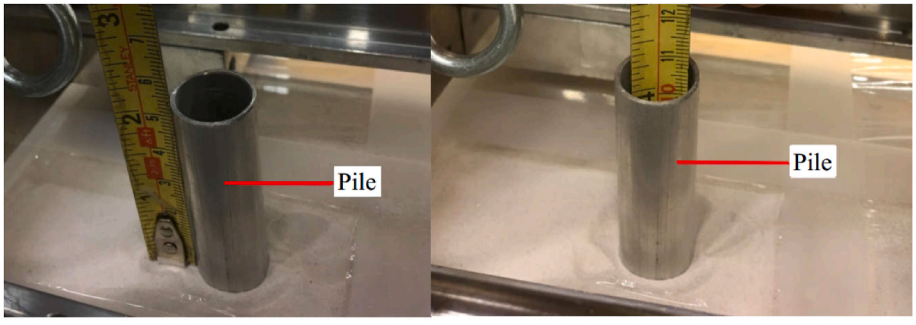

(a) (b)

Fig. 11. Soil plug analysis: (a) pile embedment length measurement; (b) soil plug length measurement. Note: A layer of plastic film has been added to the surface to prevent the sand particles dispersing during centrifuge operation.

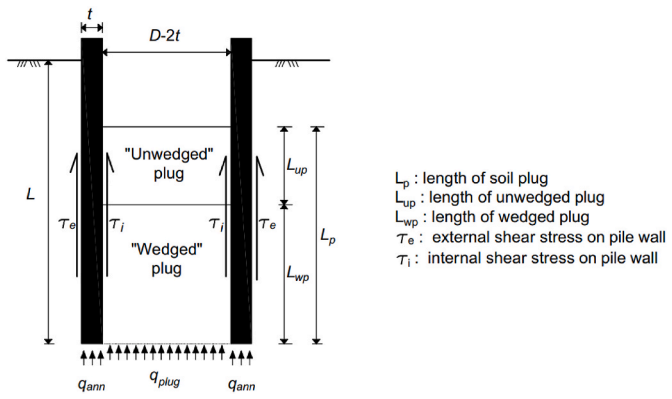

Fig. 13. Equilibrium of soil plug (modified after Lehane and Gavin, 2001).

lateral loading tests, were performed on piles that were installed at 50*g* and 1*g*. Dry sand was used to form the soil matrix, in both dense ($D_r = 80$ %) and medium-dense states ($D_r = 50$ %). Soil plug effects were studied, and the influence on pile loading behaviour was analyzed. The conclusions drawn from this study are summarized as follows.

1. The influence of loading rate on the vertical and lateral stiffness and resistance of piles during quasi-static vertical and lateral loading tests in dry sand is minimal. In both dense and medium-dense sand, a 2*D* length of in-flight installation is sufficient for piles to mobilize the desired vertical resistance (when the initial installation length was conducted at 1*g*).
2. To avoid boundary effects related to vertical loading tests in fine sand, a distance of 2.4*D* from the toe of the pile to the bottom of the centrifuge strongbox could be considered as the minimum requirement.
3. The generally accepted vertical load capacity criteria (vertical load at vertical displacement of 0.1*D*) potentially needs to be re-evaluated in medium-dense sand under different installation stresses, as it provides different values for 50*g* installed and 1*g* installed piles.
4. The level of installation stress has a more significant impact on the vertical loading behaviour, and a relatively smaller impact on the lateral loading behaviour. The lateral resistance of the 50*g* installed pile is generally 11 % higher than that of the 1*g* installed pile, in both dense and medium-dense sand.
5. The soil plug ratio of the 50*g* installed pile is much smaller than the 1*g* installed pile. This possibly leads to a stronger arching effect in the soil plug, higher post-installation soil stress state near the pile column, and formation of denser sand conditions, especially surrounding the annulus of the pile toe. This potentially results in the larger vertical and lateral stiffness and resistance for the 50*g* installed piles compared to the 1*g* installed piles.

In this study, a comparison of the loading behaviour between 50*g* installed piles and 1*g* installed piles (by jacking) has been conducted. It is important to note that the findings presented in this paper provide reference results for jacked piles but may not be fully applicable to piles installed using other techniques, such as by impact-driving or torsion-vibration, even though jacking in the centrifuge is assumed to be representative of impact-driving in the field. It is also recommended to take into consideration factors such as the presence of pore fluids in saturated conditions and cyclic loading characteristics in future research. Furthermore, in recent decades there has been a trend of increasingly large OWTs being installed, leading to increases in pile diameter and decreasing pile *L/D* ratios. The focus of the present research is on piles with a *L/D* ratio of 5, as this is still very representative of most installed piles to date. A variation of pile *L/D* ratios should be analyzed to understand if installation stress levels affect the vertical and lateral resistance and stiffness characteristics.

CRediT authorship contribution statement

Qiang Li: Writing – original draft, Software, Methodology, Investigation, Conceptualization. **Qunchao Ma:** Visualization, Software. **Xinglei Cheng:** Writing – review & editing, Visualization, Investigation. **Kenneth Gavin:** Supervision, Funding acquisition. **Luke J. Prendergast:** Writing – review & editing, Methodology. **Amin Askarinejad:** Supervision, Investigation, Funding acquisition, Conceptualization.

Data Availability Statement

Not applicable.

Funding

National Natural Science Foundation of China (NSFC) (Grant No. 52108334 and 52378361). Zhejiang Engineering Research Centre of Intelligent Urban Infrastructure (IUI2023-ZD-02). Zhejiang Provincial Science and Technology Innovation Program (New Young Talent Program) for College Students (2024R403C097). China Scholarship Council (CSC). Section of Geo-Engineering, TU Delft.

Declaration of competing interest

The authors declare that they have no known competing financial interests or personal relationships that could have appeared to influence the work reported in this paper.

Acknowledgements

The authors would like to acknowledge the support of the Key Laboratory of Soft Soil Engineering Character and Engineering Environment of Tianjin, Tianjin Chengjian University, the Section of Geo-Engineering, Delft University of Technology, and the funding from the CSC.

References

Askarinejad, A., Wang, H., Chortis, G., Gavin, K., 2022. Influence of scour protection layers on the lateral response of monopile in dense sand. Ocean Eng. 244, 110377.
Byrne, B.W., McAdam, R.A., Burd, H.J., Houlsby, G.T., Martin, C.M., Gavin, K., Doherty, P., Igoe, D., Zdravković, L., Taborda, D.M.G., Potts, D.M., Jardine, R.J., Sideri, M., Schroeder, F.C., Muir Wood, A., Kallehave, D., Skov Gretlund, J., 2015. Field testing of large diameter piles under lateral loading for offshore wind applications. In: Proceedings of the XVI. ECSMGE Geotechnical Engineering for Infrastructure and Development, pp. 1255–1260.
Byrne, B.W., Burd, H.J., Zdravkovic, L., McAdam, R.A., Taborda, D.M., Houlsby, G.T., et al., 2019. PISA: new design methods for offshore wind turbine monopiles. Rev. Fr. Geotech. 158 (3).
Byrne, B.W., 2021. Lateral pile design for offshore wind turbines. In: Piling 2020: Proceedings of the Piling 2020 Conference. ICE Publishing, pp. 13–33.
Cheng, X.L., El Naggar, M.H., Lu, D.C., Wang, P.G., Tu, W.B., 2022. A cyclic p-y elastoplastic model applied to lateral loaded pile in soft clays. Can. Geotech. J. 60 (6), 885–901.
Cheng, X.L., Liu, M.M., Li, Q., Lu, D.C., Du, X.L., 2025. Dynamic response and fatigue damage analysis of offshore wind turbines supported by four-pile jacket in clays under typhoons. Acta Geotech. 2025, 1–21.
Cheng, X.L., Wang, T.J., Zhang, J.X., Wang, P.G., Tu, W.B., Li, W.Q., 2023. Dynamic response analysis of monopile offshore wind turbines to seismic and environmental loading considering the stiffness degradation of clay. Comput. Geotech. 155, 105210.
Cheng, X.L., Li, Y., Mu, K., El Naggar, M.H., Zhou, Y., Wang, P., Liu, J., 2024. Seismic response of tripod suction bucket foun-dation for offshore wind turbine in sands. Soil Dynam. Earthq. Eng. 177, 108353.
Choo, Y.W., Kim, D., 2016. Experimental development of the p-y relationship for large-diameter offshore monopiles in sands: centrifuge tests. J. Geotech. Geoenviron. Eng. 142 (1), 04015058.
De Nicola, A., 1996. The Performance of Pipe Piles in Sand. University of Western Australia, Perth, Australia. Doctoral dissertation.
De Nicola, A., Randolph, M.F., 1997. The plugging behaviour of driven and jacked piles in sand. Geotechnique 47 (4), 841–856.
DNV, 2014. Design of Offshore Wind Turbine Structures. Offshore Standard DNV-OS-J101.

Duan, N., Cheng, Y., Liu, J., 2018. DEM analysis of pile installation effect: comparing a bored and a driven pile. Granul. Matter 20, 36.
Dyson, G.J., Randolph, M.F., 2001. Monotonic lateral loading of piles in calcareous sand. J. Geotech. Geoenviron. Eng. 127 (4), 346–352.
Fan, S., Bienen, B., Randolph, M.F., 2019. Centrifuge study on effect of installation method on lateral response of monopiles in sand. Int. J. Phys. Model. Geotech. 1–13.
Garnier, J., Gaudin, C., Springman, S.M., Culligan, P., Goodings, D., Konig, D., Kutter, B., Phillips, R., Randolph, M., Thorel, L., 2007. Catalogue of scaling laws and similitude questions in geotechnical centrifuge modelling. Int. J. Phys. Model. Geotech. 7 (3), 1–23.
Gerolymos, N., Escoffier, S., Gazetas, G., Garnier, J., 2009. Numerical modeling of centrifuge cyclic lateral pile load experiments. Earthq. Eng. Eng. Vib. 8, 61–76.
Henke, S., Grabe, J., 2008. Numerical investigation of soil plugging inside open-ended piles with respect to the installation method. Acta Geotechnica 3 (3), 215–223.
Henke, S., Bienen, B., 2013. Investigation of the influence of the installation method on the soil plugging behaviour of a tubular pile. In: ICPMG2014-Physical Modelling in Geotechnics, vol. 2. CRC Press, Leiden, the Netherlands, pp. 681–687.
Klinkvort, R.T., Hededal, O., 2010. Centrifuge modelling of offshore monopile foundation. In: Frontiers in Offshore Geotechnics II: Proceedings of the 2nd International Symposium Frontiers in Offshore Geotechnics (ISFOG2010). Taylor and Francis, London, UK, pp. 581–586.
Klinkvort, R.T., Hededal, O., 2013. Lateral response of monopile supporting an offshore wind turbine. Proc. Inst. Civ. Eng. Geotech. Eng. 166 (2), 147–158.
Klinkvort, R.T., Hededal, O., 2014. Effect of load eccentricity and stress level on monopile support for offshore wind turbines. Canad. Geotech. J. 51 (9), 966–974.
Komusanac, I., Brindley, G., Fraile, D., Ramirez, L., 2021. Wind Energy in Europe. Statistics and the Outlook for 2022-2026. Issue.
Krapfenbauer, C., 2016. Experimental Investigation of Static Liquefaction in Submarine Slopes. TU Delft. MSc Thesis.
Labenski, J., Moormann, C., Aschrafi, J., Bienen, B.W., 2016. Simulation on the plug inside open steel pipe piles with regards to different installation methods. In: Proceedings of 13th Baltic Sea Geotechnical Conference. Vilnius Gediminas Technical University, Vilnius, Lithuania, pp. 223–230.
LeBlanc, C., Houlsby, G.T., Byrne, B.W., 2010. Response of stiff piles in sand to long-term cyclic lateral loading. Geotechnique 60 (2), 79–90.
Lee, J., 2008. Experimental Investigation of the Load Response of Model Piles in Sand. Purdue University. PhD thesis.
Lehane, B.M., Gavin, K.G., 2001. Base resistance of jacked pipe piles in sand. J. Geotech. Geoenviron. Eng. 127 (6), 473–480.
Li, Z., Haigh, S.K., Bolton, M.D., 2010a. Centrifuge modelling of mono-pile under cyclic lateral loads. Phys. Model. Geotech 965–970.
Li, Z., Haigh, S.K., Bolton, M.D., 2010b. The response of pile groups under cyclic lateral loads. Int. J. Phys. Model. Geotech. 10 (2), 47–57.
Li, Q., Askarinejad, A., Gavin, K., 2020a. Lateral response of rigid monopiles subjected to cyclic loading: centrifuge modelling. Proceedings of the Institution of Civil Engineers - Geotechnical Engineering 1–35.
Li, Q., Prendergast, L.J., Askarinejad, A., Chortis, G., Gavin, K., 2020b. Centrifuge modeling of the impact of local and global scour erosion on the monotonic lateral response of a monopile in sand. Geotech. Test. J. 43, 1084–1100.
Li, Q., Prendergast, L.J., Askarinejad, A., Gavin, K., 2020c. Influence of vertical loading on behavior of laterally-loaded foundation piles: a review. J. Mar. Sci. Eng. 8 (12), 1029.
Li, Q., Gavin, K., Askarinejad, A., Prendergast, L.J., 2022. Experimental and numerical investigation of the effect of vertical loading on the lateral behaviour of monopiles in sand. Can. Geotech. J. 59 (5), 652–666.
Li, Q., Diao, H., Ma, Q., Wang, K., Wang, X., Wang, M., 2024a. Geospatial analysis of scour development in offshore wind farms. Mar. Georesour. Geotechnol. (online).
Li, Q., Prendergast, L.J., Gavin, K.G., Askarinejad, A., Wang, X., 2024b. A method to quantify the beneficial effect of scour protection on lateral behaviour of monopiles for offshore wind turbines. Ocean Eng. 307.
Liu, H., Nagula, S., Jostad, H.P., Piciullo, L., Nadim, F., 2024. Considerations for using critical state soil mechanics based constitutive models for capturing static liquefaction failure of tailings dams. Comput. Geotech. 167, 106089.
Lu, W., Zhang, G., 2018. Influence mechanism of vertical-horizontal combined loads on the response of a single pile in sand. Soils Found. 58 (5), 1228–1239.
Ma, C., Ban, J., Zi, G., 2024. Comparative study on the dynamic responses of monopile and jacket-supported offshore wind turbines considering the pile-soil interaction in transitional waters. Ocean Eng. 292, 116564.
Maghsoudloo, A., Askarinejad, A., De Jager, R.R., Molenkamp, F., Hicks, M.A., 2018. Experimental investigation of pore pressure and acceleration development in static liquefaction induced failures in submerged slopes. In: 9th International Conference of Physical Modelling in Geotechnics. London, UK.
Mahutka, K.P., König, F., Grabe, J., 2006. Numerical modelling of pile jacking, driving and vibratory driving. In: Proceedings of International Conference on Numerical Simulation of Construction Processes in Geotechnical Engineering for Urban Environment (NSC06), pp. 235–246. Rotterdam, the Netherlands.
Mu, L., Kang, X., Feng, K., Huang, M., Cao, J., 2018. Influence of vertical loads on lateral behaviour of monopiles in sand. Eur. J. Environ. Civ. Eng. 22 (Suppl. 1), 286–301.
Nunez, I.L., Hoadley, P.J., Randolph, M.F., 1988. Driving and tension loading of piles in sand on a centrifuge. In: Proceedings of the International Conference Centrifuge, pp. 353–362.
Ovesen, N.K., 1979. The scaling law relationships. Proceedings of 7th Europe Conference Soil Mechanics and Foundation Engineering 4, 319–323. Brighton.
Phuong, N.T.V., van Tol, A.F., Elkadi, A.S.K., Rohe, A., 2016. Numerical investigation of pile installation effects in sand using material point method. Comput. Geotech. 73, 58–71.
Prakasha, K., Joer, H., Randolph, M., 2005. Establishing a model testing capability for deep water foundation systems. In: Proceedings of the 15th International Offshore and Polar Engineering Conference and Exhibition, pp. 309–315. Seoul, Korea.
Qi, W., Gao, F., Randolph, M., Lehane, B., 2016. Scour effects on p-y curves for shallowly embedded piles in sand. Geotechnique 66 (8), 648–660.
Randolph, M.F., Leong, E.C., Houlsby, G.T., 1991. One dimensional analysis of soil plugs in pipe piles. Geotechnique 41 (4), 587–598.
Richards, I.A., Bransby, M.F., Byrne, B.W., Gaudin, C., Houlsby, G.T., 2021. Effect of stress level on response of model monopile to cyclic lateral loading in sand. J. Geotech. Geoenviron. Eng. 147 (3).
SibelcoEurope, 2016. Technical Data: Geba Sand. Eurogrit BV.
Stein, P., Hinzmann, N., Gattermann, J., 2018. Scale model investigations on vibro pile driving. ASME 2018 37th International Conference on Ocean. Offshore and Arctic Engineering.
Sørensen, S.P.H., Ibsen, L.B., 2013. Assessment of foundation design for offshore monopiles unprotected against scour. Ocean Eng. 63, 17–25.
Truong, P., Lehane, B., Zania, V., Klinkvort, R.T., 2018. Empirical Approach Based on Centrifuge Testing for Cyclic Deformations of Laterally Loaded Piles in Sand.
Verdure, L., Garnier, J., Levacher, D., 2003. Lateral cyclic loading of single piles in sand. Int. J. Phys. Model. Geotech. 3 (3), 17–28.
Wen, K., Wu, X., Zhu, B., 2020. Numerical investigation on the lateral loading behaviour of tetrapod piled jacket foundations in medium dense sand. Appl. Ocean Res. 100, 102193.
Wen, K., Liu, T., Zhu, B., Liu, D., 2023. Torque-transferring characteristics of offshore tetrapod piled jacket foundations in dense sand. Int. J. GeoMech. 23 (3), 04023002.
Wen, K., Cerfontaine, B., White, D., Gourvenec, S., Diambra, A., 2024a. Lateral bearing factors and elastic stiffness factors for robotic CPT p-y module in undrained clay. Comput. Geotech.
Wen, K., Jardine, R.J., Kontoe, S., Liu, T., 2024b. Finite element modelling of driven pipe piles in the low-to-medium density chalk under axial monotonic loading. Comput. Geotech.
Wang, H., van Zanten D, V., de Lange, D., Pisanò, F., Gavin, K., Askarinejad, A., 2022. Centrifuge study on the CPT based p-y models for the monopiles. The 5th International Symposium on Cone Penetration Testing. CPT'22. Bologna, Italy.
Yang, Q., Gao, Y., Kong, D., Zhu, B., 2019. Centrifuge modelling of lateral loading behaviour of a "semi-rigid" monopile in soft clay. Mar. Georesour. Geotechnol. 37 (10), 1205–1216.
Yoo, M.T., Choi, J.I., Han, J.T., Kim, M.M., 2013. Dynamic p-y curves for dry sand from centrifuge tests. J. Earthq. Eng. 17 (7), 1082–1102.
Zhang, W., Askarinejad, A., 2019. Behaviour of buried pipes in unstable sandy slopes. Landslides 16 (2), 283–293.
Zhu, B., Wen, K., Kong, D., Zhu, Z., Wang, L., 2018. A numerical study on the lateral loading behaviour of offshore tetrapod piled jacket foundations in clay. Appl. Ocean Res. 75, 165–177.
Zhu, B., Wen, K., Li, T., Wang, L., Kong, D., 2019. An experimental study on the lateral pile-soil interaction of tetrapod piled jacket foundations in sand. Can. Geotech. J. 56 (11), 1680–1689.